Nonlinear Functional Analysis and Applications
Vol. 31, No. 1 (2026), pp. 259-284
ISSN: 1229-1595(print), 2466-0973(online)

https://doi.org/10.22771/nfaa.2026.31.01.17
http://nfaa.kyungnam.ac.kr/journal-nfaa

CONSTRUCTION OF NON-STANDARD FINITE DIFFERENCE METHOD FOR SOLVING JUMARIE TYPE FRACTIONAL DIFFERENTIAL MODEL USING MICKENS SCHEME

Said Al Kathiri[1], Altaf A Bhat[2] and Danish A Sunny[3]

[1]Sciences and Mathematics Unit, Department of Supportive Requirements, UTAS, Salalah, Sultanate of Oman
e-mail: said.alkathiri@utas.edu.om

[2]Sciences and Mathematics Unit, Department of Supportive Requirements, UTAS, Salalah, Sultanate of Oman
e-mail: altaf@utas.edu.om

[3]Sciences and Mathematics Unit, Department of Supportive Requirements, UTAS, Salalah, Sultanate of Oman
e-mail: danish.sunny@utas.edu.om

Abstract. In this paper we construct Non-standard finite difference scheme (NSFDS) for the Jumarie type fractional differential system in-terms of Mittag-Leffler function by using Mickens scheme given in the literature by Roegers. After developing this method, the algorithm is applied in physical system of fractional differential equations. The analytical results obtained are then compared with the numerical solutions by using error graphs and heat map graphs. The efficiency of the scheme is established as it aligns with the exact solution precisely. We also use convergence maps for the NSFDS by showing faster convergence as we decrease the step size.

1. Introduction

Fractional calculus, an extension of ordinary calculus, has created a new mathematical method for resolving problems in a number of fields, such as quantitative biology, control theory, probability, and more. These phenomena

[0]Received November 1, 2025. Revised December 4, 2025. Accepted December 13, 2025.
[0]2020 Mathematics Subject Classification: 34A30, 65L07.
[0]Keywords: Fractional calculus, Jumarie fractional derivative, Mittag-Leffler function, fractional differential equations, nonstandard finite difference scheme, stability analysis.
[0]Corresponding author: Altaf A Bhat(altaf@utas.edu.om).

are better represented by differential equations. Certain fractional calculus equations that capture these events have been solved using the characteristics of well-known fractional calculus. The majority of these differ-integral equations have solutions in the form of Fox-Wright functions, Mittag-Leffler functions, etc.

Fractional calculus is defined by a variety of researchers. The most commonly definition that is used is the Riemann-Liouvellie (R-L) definition [14,15, 29,35,41]. The fractional derivative in terms of Caputo is one of the other helpful definitions [14,15,29,35,41]. The left-hand variant provided by Jumarie for the fractional derivative suggested by Riemann-Liouvellie is useful in order to avoid a constant function having a nonzero fractional derivative [28]. A hypothesis of characterizing non-differentiable points using a right-handed version of Jumarie's fractional derivative of the fractional derivative proposed by Riemann-Liouvellie was recently proposed by Ghosh et al. [23]. Differential equations in different fractional derivative forms yield distinct kinds of solutions [14,15,29,35,41]. As a result, a standard algorithm cannot solve fractional differential equations. Therefore, one of the emerging areas of applied mathematics is the interpretation and solution of FDE's. To solve both linear and non-linear differential equations, several techniques have been used and developed recently, including the Predictor-Corrector approach [16], Homotopy Perturbation method [1], Adomain decomposition method [27,41,44], Differential transform method [21], and Variational Iteration method [49]. Ghosh et al. have developed an analytical method for solving linear FDEs with Jumarie's derivative [28] by utilizing Mittag-Leffler functions and generalized sine and cosine functions in [24].

The power series method created by Rida [45] and the AdamsBashforth method introduced by Diethelm [17] are two numerical approaches that have demonstrated some efficacy, while Zeid [50] offered a thorough analysis of the methods that are now accessible. Because of their computational efficiency and ease of use, finite difference methods, or FDMs, are widely utilized. However, typical FDMs may have serious problems when applied to fractional-order systems, especially coupled nonlinear systems. These problems could include inadequate convergence, loss of stability, or an inability to reproduce the qualitative behavior of the original system. In order to get over these restrictions, Mickens [32,33] developed the Nonstandard Finite Difference (NSFD) approach, which has turned out to be an effective substitute. In order to maintain the essential qualitative characteristics of the original continuous system, such as positivity, boundedness, equilibrium stability, and dynamical consistency, NSFD schemes are built utilizing modelling techniques. In contrast to conventional FDMs, NSFD methods frequently make use of nonlocal approximations and specially designed denominator functions that are adapted to

the nature of the problem. The modelling foundation of NSFDs was further enhanced by Mickens' introduction of the concept of precise schemes.

Numerous NSFD approach applications to chaotic and nonlinear fractional systems have been documented in [46,47]. Using the GrunwaldLetnikov approximation, Moaddy [37] employed NSFD to examine the chaotic dynamics of the fractional-order Rossler system. Ongun [38] effectively reproduced the intricate behaviour of the fractional-order Brusselator model by applying NSFD to it. NSFD techniques were expanded by Hajipour [26] and others to novel systems incorporating Caputo derivatives and nonlinearities [6] as well as chaotic fractional systems like the Chen system [48].

However, the application of NSFD approaches to fractional systems with real and complex eigenvalues has been the subject of very few studies. The long-term behaviour and asymptotic stability of this class of systems are highly susceptible to numerical approximation, which poses a considerable problem. Standard finite difference techniques typically destabilize otherwise stable continuous systems or result in numerical artifacts in these systems. Thus, it is imperative to develop NSFD techniques specifically designed to handle real and complex-eigenvalue systems and ensure that their dynamics are accurately represented across time. For instance, the fractional logistic model was solved using the new iterative approach [8] and the homotopy perturbation method, which were not constrained by the carrying capacity of the model. As a result, they are not dynamically consistent. Samah et al. [2] provided the NSFDM for solving a Caputo-type fractional linear system having real eigenvalues.

Nonstandard finite difference methods offer distinct advantages over traditional finite difference approaches since they can produce exact numerical schemes that yield precise solutions at the nodal points. Micken was the pioneer in formulating and explaining the derivation of exact finite difference methods aimed at solving particular types of first-order differential equations, including logistic and exponential growth, systems of linear ODE models, higher-order ODEs, and specific PDE challenges, among others [7,31]. Nonstandard finite difference schemes were originally developed to deliver either a highly accurate finite difference scheme or the most efficient numerical scheme to capture all the qualitative aspects of the exact solution to the original problem.

Applications of the nonstandard finite difference method to a fractional model are examined explaining diabetes mellitus and its complications [3]. Altaf et al. [9] introduced and presented the generating operators for I-transform together with the corresponding operational relations.Volterra q-integral equations are solved by using the method of q-differential transformation by Altaf et al. [10]. Exact solutions of linear and nonlinear q-integral

equations have been investigated. Some new investigations have been done in [39,43] based on fractional integral inequalities and fractional order transforms.

A cholera delay model is discussed for equilibria in presence of the delay parameter a priori existence and uniqueness [4]. Modulation equations are developed for systems with dual Turing instabilities, providing rigorous approximation and attractivity results in the presence of 1:2 wave number ratios [22]. An upgraded chaotic Pan system with hidden and self-excited hyperchaotic attractors is analyzed, with analytical conditions for supercritical Hopf bifurcations supported by simulations [5].

The goal of this paper is to provide a method numerically for solving two-dimensional FDE's using nonstandard finite difference discretisation. It contrasts the suggested scheme's performance with alternative approaches from the literature. The key characteristics of the suggested numerical method include unconditional stability, high order of convergence, and explicit Euler method-like design. The infinity norm is used to assess and gauge the approximation mistakes of procedure, which are very small and fall inside or very close to the machine precision.

This is how the remainder of the paper is structured. An introduction to calculus of fractional (FC) and the creation of a non-standard scheme utilizing Mickens principles are given in Section 1. The preliminary mathematical information is provided in section 2. The suggested methodology is presented in Section 3. In order to assess the efficacy of the suggested method, Section 4 uses numerical examples from the contents of current literature. After that, the results are contrasted with those of other approaches that have been discussed in the literature. Lastly, Section 5 presents the discussions and conclusions.

2. Mathematical preliminaries

Definition 2.1. The left Riemann-Liouville (R-L) definition of fractional derivative is given as follows:

$$ {}_bD_z^{\alpha} f(z) = \frac{1}{\Gamma(n+1-\alpha)} \left(\frac{d}{dz}\right)^{n+1} \int_b^z (z-t)^{n-\alpha} f(t) dt, \tag{2.1} $$

where α lies between n and $n+1$, n is positive integer.
If we take $0 \leq \alpha < 1$, then

$$ {}_bD_z^{\alpha} f(z) = \frac{1}{\Gamma(1-\alpha)} \frac{d}{dz} \int_b^z (z-t)^{-\alpha} f(t) dt. \tag{2.2} $$

Consequently, the right R-L fractional derivative is:

$$ {}_{z}D_{b}^{\alpha} f(z) = \frac{1}{\Gamma(1-\alpha)} \frac{-d}{dz} \int_{z}^{b} (\tau - z)^{m-\alpha} f(\tau) d\tau, \tag{2.3} $$

where $n \leq \alpha < n+1$.

In contrast to a constant's classical derivative of zero, the derivative of a constant is non-zero, as defined by definitions (2.1)(2.3) above. To overcome this limitation, Caputo [12] proposed a version of the R-L idea of fractional derivative in 1967.

Definition 2.2. Fractional derivative given by Caputo is as follows [12]:

$$ {}_{b}^{C}D_{z}^{\alpha} f(z) = \frac{1}{\Gamma(m-\alpha)} \int_{b}^{z} (z-t)^{m-\alpha-1} f^{m}(t) dt, \tag{2.4} $$

where $m-1 \leq \alpha < m$.

This idea involves differentiating $f(x)$ n times initially, followed by the integration of $n-\alpha$ times. The disadvantage of this approach is that the α-th order derivative, in this case $m-1 \leq \alpha < m$, cannot exist unless $f(x)$ is n times differentiable. If the function is non-differentiable, this definition is not applicable. There are two main benefits to this approach: (i) the constant has a fractional derivative of zero; and (ii) the R-L type differential equations have fractional type initial conditions, in the case of Caputo type fractional differential equations, the initial conditions are in accordance with the classical derivative type.

Accordingly, a fractional differential equation involving R-L fractional derivatives requires knowledge of fractional beginning conditions, which are sometimes difficult to physically grasp [14].

Definition 2.3. Jumarie [28] introduced a different approach to characterize the left R-L type fractional derivative of the function f(x) over the interval [a,b], aiming to address the issue of the fractional derivative of a non-zero constant.

$$ f_{L}^{(\alpha)}(z) = {}_{a}^{J} D_{z}^{\alpha} f(z) \begin{cases} \frac{1}{\Gamma(-\alpha)} \int_{a}^{z} (z-t)^{-\alpha-1} f(t) dt, & \alpha < 0, \\ \frac{1}{\Gamma(1-\alpha)} \frac{d}{dz} \int_{a}^{z} (z-t)^{-\alpha} (f(t) - f(a)) dt, & 0 < \alpha < 1, \\ \left(f^{(\alpha-n)}(z) \right)^{(n)}, & n \leq \alpha < n+1. \end{cases} \tag{2.5} $$

They assume that $f(z) - f(a) = 0$ for $z < a$. The second line of equation (2.5) displays the R-L derivative of the offset function of order $0 < \alpha < 1$, or $f(x) - f(a)$, whereas the first statement expresses the fractional integration. They use the third line for $\alpha > 1$, which indicates that after differentiating

the offset function of order $0 < \alpha - n < 1$ using the formula of the second line, they apply complete n order differentiation to it. The integer n, which is slightly smaller than the real number α $(n \leq \alpha < n + 1)$, was chosen in this instance.

Definition 2.4. Mittag-Leffler introduced and explored the Mittag-Leffler function, which serves as a generalization of the exponential function. The function e^x is specifically extended by this function, which plays a crucial role in the field of fractional calculus. The following representations of Mittag-Leffler functions with up to three parameters have been developed using power series expansion [30,36,42].

$$E_\alpha(x) = \sum_{i=0}^{\infty} \frac{x^i}{\Gamma(1+\alpha i)}, \text{ for } \alpha \in C, Re(\alpha) \textit{ is positive.} \tag{2.6}$$

$$E_{\alpha,\beta}(x) = \sum_{i=0}^{\infty} \frac{x^i}{\Gamma(\beta+\alpha i)}, \text{ for } \alpha, \beta \in C, Re(\alpha) \textit{ is positive.} \tag{2.7}$$

$$E^{\gamma}_{\alpha,\beta}(x) = \sum_{i=0}^{\infty} \frac{(\gamma)_i x^i}{\Gamma(\beta+\alpha i) i!}, \text{ for } \alpha, \beta, \gamma \in C, Re(\alpha) \textit{ is positive.} \tag{2.8}$$

where, $(\gamma)_j = \gamma(\gamma+1)(\gamma+2)(\gamma+3)...(\gamma+j-1)$ and $(\gamma)_0 = 1$.

[18,19,20,36] described and gave the integral representation of the Mittag-Leffler function as follows:

$$E_\alpha(z) = \frac{1}{2\pi} \int_C \frac{t^{\alpha-1} e^t}{t^\alpha - z} dt, \ z \in \mathbb{C}, \ Re(\alpha) \textit{ is positive.}$$

In this case, C is a loop that encloses the disk's circles $|t| \leq |z|^{1/\alpha}$ in the +ive sense: $|arg(t)| \leq \pi$ on the contour C [18,19,20,36]. It begins and ends at $-\infty$. The two parameter Mittag-Leffler function's appropriate integral representation is provided by [18,19,20,36] as follows:

$$E_{\alpha,\beta}(z) = \frac{1}{2\pi} \int_C \frac{t^{\alpha-\beta} e^t}{t^\alpha - z} dt, \ z \in \mathbb{C}, \ Re(\alpha) \textit{ is positive,}$$

where C, the contour is same as above.

3. Development of two dimensional non-standard finite difference methods

In this section, we develop NSFDM for solving the system of two dimensional FDE's.

Consider the FDE's in the linear system:

$$\begin{cases} {}^{J}D^{\alpha}[x] = px + qy, \\ {}^{J}D^{\alpha}[y] = rx + sy. \end{cases} \tag{3.1}$$

Here p, q, r and s are the constants, ${}^{J}D^{\alpha}$ is the Jumarie's fractional operator, we call this for convenience ${}^{J}D^{\alpha} = \frac{d^{\alpha}}{dt^{\alpha}}$, and x, y are functions of t.The parameters here represent the rate at which the quantity diminishes. These provides an intuitive measure of how long a system persists before significant reduction.Limitations include absence of ecological and environmental factors. Ghosh et al. [25] derived the solution of the system as follows:

$$\begin{cases} x(t) = AE_{\alpha}(\lambda t^{\alpha}), \\ y(t) = BE_{\alpha}(\lambda t^{\alpha}). \end{cases}$$

For the eigenvalues λ_1, λ_2, the corresponding eigenfunction is given by Ghosh et al. [25], as follows:

$$\lambda^2 - (p+s)\lambda + (ps - qr) = 0.$$

When the characteristic equation's roots are real and distinct will be covered in this section.

In recent years, nonstandard finite-difference (NSFD) methods have gained popularity Mickens [31,32,33] and Patidar [40], mostly due to the fact that some of these methods are more effective at maintaining specific qualitative characteristics in the original differential equations or systems. Patidar [40] provides an excellent overview of NSFD techniques. Understanding the precise finite-difference methods is a good place to start because NSFD methods require a solid theoretical foundation [32]. Mickens's works have shown some positive outcomes [31,32,33]. It can be demonstrated that, depending on the step sizes selected, accurate finite-difference algorithms can take on several shapes. Dalir & Bashour [13] and Mickens et al. [34] have developed many accurate finite-difference approaches for the linear 2nd-order equation with constant coefficients.

We examine a linear system of fractional differential equations (3.1) that are connected and have constant coefficients.

For the sake of notations, let

$$x_{m+n} = x(t + nh),\ x_m = x(t),\ y_{m+n} = y(t + nh),\ y_m = y(t).$$

The fractional system (3.1) is also represented as $Y' = AY$, where $Y = (x, y)^T$ and A is the matrix of coefficients.

Micken's [32] demonstrated that the exact finite-difference technique can be expressed in the following form if the eigenvalues are of the coefficient matrix

are $\lambda_{1,2} = (p+s)n\sqrt{(p+s)^2 - 4(ps-qr)}$, for the general fractional system (3.1) when $ps - qr \neq 0$.

$$\begin{cases} \frac{x_{k+1}-\Psi_{xk}}{\Phi} = px_k + qy_k, \\ \frac{y_{k+1}-\Psi_{xk}}{\Phi} = rx_k + sy_k. \end{cases} \tag{3.2}$$

This fractional linear system can be defined as follows:

$$\mathbf{w}' = J\mathbf{w}, \tag{3.3}$$

where

$$J = \begin{bmatrix} \lambda_1 & 0 \\ 0 & \lambda_2 \end{bmatrix}.$$

The solution for this system is the exact finite-difference scheme, which is as follows:

$$\frac{1}{\Phi}(\mathbf{w}_{k+1} - \mathbf{w}_k) = J[\theta\mathbf{w}_{k+1} + (1-\theta)\mathbf{w}_k], \tag{3.4}$$

where $\mathbf{w}_{k+1} = \mathbf{w}(t+h)$ and $\mathbf{w}_k = \mathbf{w}(t)$. Here, ϕ and θ depends on the eigenvalues of the system. Three cases arise, which are as follows:

Case i: If the eigenvalues are real and different, then the ϕ and θ are defined as follows:

$$\phi = \frac{(\lambda_1 - \lambda_2)(E_\alpha(\lambda_1 h)^\alpha - 1)(E_\alpha(\lambda_2 h)^\alpha - 1)}{\lambda_1\lambda_2\Big(E_\alpha(\lambda_1 h)^\alpha - E_\alpha(\lambda_2 h)^\alpha\Big)}$$

and

$$\theta = \frac{\lambda_2\Big(E_\alpha(\lambda_1 h)^\alpha - 1\Big) - \lambda_1\Big(E_\alpha(\lambda_2 h)^\alpha - 1\Big)}{(\lambda_1 - \lambda_2)\Big(E_\alpha(\lambda_1 h)^\alpha - 1\Big)\Big(E_\alpha(\lambda_2 h)^\alpha - 1\Big)}.$$

The method (3.3) is valid when two eigenvalues are different as $\lambda_1 - \lambda_2$ lies in denominators of Φ and Ψ, this is possible only if $\lambda_1 \neq \lambda_2$. Also since $ps - qr \neq 0$, none of the eigenvalues are zero, $\lambda_1\lambda_2 \neq 0$.

Case ii: If the eigenvalues are the same, then the θ and ϕ are given as follows:

$$\phi = \frac{(E_\alpha(\lambda h)^\alpha - 1)^2}{\lambda^2 h\Big(E_\alpha(\lambda h)\Big)}$$

and

$$\theta = \frac{1 - E_\alpha(\lambda h) + \lambda h E_\alpha(\lambda h)}{\Big(E_\alpha(\lambda h) - 1\Big)^2}.$$

Case iii: If the eigenvalues are complex, then the ϕ and θ are defined as follows:

$$\phi = \frac{b\Big(E_\alpha(2ah) + 1 - 2E_\alpha(ah)\ cos(bh))\Big)}{(a^2+b^2)E_\alpha(ah)\ sin(bh)}$$

and

$$\theta = \frac{b + aE_\alpha(ah)\ sin(bh) - bE_\alpha(ah)\ cos(bh)}{b\Big(E_\alpha(2ah) + 1 - 2E_\alpha(ah)\ cos(bh)\Big)}.$$

4. Applications of the proposed schemes

In this section we applied the Micken's method, developed above, on four examples. All the examples represent real applications. They represent different cases of growth and decay scenarios based on classification of eigen values. which are as follows:

Example 4.1. Let the system of fractional differential equations be as follows:

$$\begin{cases} {}^J D^\alpha x = y + 2x \\ {}^J D^\alpha y = 2y + x \end{cases}, \ 0 < \alpha \leq 1 \ with \ y(0) = 1, \ x(0) = 2.$$

Let $x(t) = AE_\alpha(\lambda t^\alpha)$ and $y(t) = BE_\alpha(\lambda t^\alpha),\ t > 0$ be the exact solution of the above system of equations.

Then for the above system, the characteristic equation is:

$$\begin{bmatrix} 2-\lambda & 1 \\ 1 & 2-\lambda \end{bmatrix} = 0.$$

On solving the characteristic equation, we have $\lambda = 1, 3$.

Then when solving further, the solutions are as follows:

$$x(t) = E_\alpha(3t^\alpha) + E_\alpha(t^\alpha),$$
$$y(t) = E_\alpha(3t^\alpha) - E_\alpha(t^\alpha).$$

This is the exact solution of the above system of the fractional model.

Let $h = T/N$ and $N > 1 \in I$. Let $k = 0, 1, ..., N$ and $x_k = kh$. The exact solution's basis function is $E_\alpha(\lambda t^\alpha)$.

Now, we follow Micken's rules for establishing NSFD schemes. This fractional linear system can be expressed as follows:

$$\mathbf{w}' = J\mathbf{w}, \tag{4.1}$$

where

$$J = \begin{bmatrix} 3 & 0 \\ 0 & 1 \end{bmatrix}.$$

The solution for this system is the exact finite-difference scheme, which is as follows:

$$\frac{1}{\Phi}(\mathbf{w}_{k+1} - \mathbf{w}_k) = J[\theta \mathbf{w}_{k+1} + (1-\theta)\mathbf{w}_k], \tag{4.2}$$

where $\mathbf{w}_{k+1} = \mathbf{w}(t+h)$, $\mathbf{w}_k = \mathbf{w}(t)$ and ϕ with θ are defined as follows:

$$\phi = \frac{2(E_\alpha(3h)^\alpha - 1)(E_\alpha(h)^\alpha - 1)}{3\Big(E_\alpha(3h)^\alpha - E_\alpha(h)^\alpha\Big)}$$

and

$$\theta = \frac{\Big(E_\alpha(3h)^\alpha - 1\Big) - 3\Big(E_\alpha(h)^\alpha - 1\Big)}{2\Big(E_\alpha(3h)^\alpha - 1\Big)\Big(E_\alpha(h)^\alpha - 1\Big)}.$$

For the validity of this method, the two eigenvalues need to be different. Here, we have $\lambda_1 \neq \lambda_2$. Also $ps - qr \neq 0$, none of them is zero, $\lambda_1\lambda_2 \neq 0$.

Example 4.2. Suppose the system of fractional differential equations

$$\begin{cases} {}^J D^\alpha x = y - 2x \\ {}^J D^\alpha y = -2y + x \end{cases}, \ 0 < \alpha \leq 1 \ with \ y(0) = 1, \ x(0) = 2.$$

Let $x(t) = AE_\alpha(\lambda t^\alpha)$ and $y(t) = BE_\alpha(\lambda t^\alpha), \ t > 0$ be its solution.

For the above system, the characteristic equation is:

$$\begin{bmatrix} -2-\lambda & 1 \\ 1 & -2-\lambda \end{bmatrix} = 0.$$

On solving the characteristic equation, we have $\lambda = -1, -3$.

Then when solving further, the solutions are as follows:

$$x(t) = E_\alpha(-3t^\alpha) + E_\alpha(-t^\alpha),$$
$$y(t) = E_\alpha(-3t^\alpha) - E_\alpha(-t^\alpha).$$

This is the exact solution of the above system of the fractional model.

Let $h = T/N$ and $N > 1 \in I$. Let $k = 0, 1, ..., N$ and $x_k = kh$. The exact solution's basis function is $E_\alpha(\lambda t^\alpha)$.

Now, we follow the Micken's rules for establishing NSFD schemes. This fractional linear system can be expressed as follows:

$$\mathbf{w}' = J\mathbf{w}, \tag{4.3}$$

where

$$J = \begin{bmatrix} -3 & 0 \\ 0 & -1 \end{bmatrix}.$$

The solution for this system is the exact finite-difference scheme, which is as follows:

$$\frac{1}{\Phi}(\mathbf{w}_{k+1} - \mathbf{w}_k) = J[\theta \mathbf{w}_{k+1} + (1-\theta)\mathbf{w}_k], \tag{4.4}$$

where $\mathbf{w}_{k+1} = \mathbf{w}(t+h)$, $\mathbf{w}_k = \mathbf{w}(t)$ and ϕ with θ are defined as follows:

$$\phi = \frac{-2(E_\alpha(-3h)^\alpha - 1)(E_\alpha(-h)^\alpha - 1)}{3\Big(E_\alpha(-3h)^\alpha - E_\alpha(-h)^\alpha\Big)}$$

and

$$\theta = \frac{-\Big(E_\alpha(-3h)^\alpha - 1\Big) + 3\Big(E_\alpha(-h)^\alpha - 1\Big)}{-2\Big(E_\alpha(-3h)^\alpha - 1\Big)\Big(E_\alpha(-h)^\alpha - 1\Big)}.$$

For the validity of this method, the two eigenvalues need to be different. Here, we have $\lambda_1 \neq \lambda_2$. Also $ps - qr \neq 0$, none of them is zero, $\lambda_1\lambda_2 \neq 0$.

Example 4.3. Let us assume system of fractional differential equations

$$\begin{cases} {}^J D^\alpha x = -y + 4x \\ {}^J D^\alpha y = 2y + x \end{cases}, \ 0 < \alpha \leq 1 \ with \ y(0) = 1, \ x(0) = 2.$$

Let $x(t) = AE_\alpha(\lambda t^\alpha)$ and $y(t) = BE_\alpha(\lambda t^\alpha), \ t > 0$ be its solution.

For the above system, the characteristic equation is:

$$\begin{bmatrix} 4-\lambda & 1 \\ 1 & 2-\lambda \end{bmatrix} = 0.$$

On solving characteristic equation, we have $\lambda = 3, 3$.

Then when solving further, the solutions are as follows:

$$x(t) = E_\alpha(3t^\alpha) + \frac{1}{\Gamma(1+\alpha)}\big[t^\alpha + \Gamma(1+\alpha)\big]E_\alpha(3t^\alpha),$$

$$y(t) = E_\alpha(3t^\alpha) + \frac{1}{\Gamma(1+\alpha)}t^\alpha E_\alpha(3t^\alpha).$$

This is the exact solution of the above system of the fractional model.

Let $h = T/N$ and $N > 1 \in I$. Let $k = 0, 1, ..., N$ and $x_k = kh$. The exact solution's basis function is $E_\alpha(\lambda t^\alpha)$.

Now, we follow the Micken's rules for establishing NSFD schemes. This fractional linear system can be expressed as follows:

$$\mathbf{w}' = J\mathbf{w}, \tag{4.5}$$

where

$$J = \begin{bmatrix} 3 & 0 \\ 0 & 3 \end{bmatrix}.$$

The solution for this system is exact finite-difference scheme, which is as follows:

$$\frac{1}{\Phi}(\mathbf{w}_{k+1} - \mathbf{w}_k) = J[\theta \mathbf{w}_{k+1} + (1-\theta)\mathbf{w}_k], \tag{4.6}$$

where $\mathbf{w}_{k+1} = \mathbf{w}(t+h)$, and $\mathbf{w}_k = \mathbf{w}(t)$ and ϕ with θ are defined as follows:

$$\phi = \frac{(E_\alpha(\lambda h)^\alpha - 1)^2}{\lambda^2 h\Big(E_\alpha(\lambda h)\Big)}$$

and

$$\theta = \frac{1 - E_\alpha(\lambda h) + \lambda h E_\alpha(\lambda h)}{\Big(E_\alpha(\lambda h) - 1\Big)^2}.$$

As the two eigenvalues are the same, $\lambda_1 = \lambda_2$, this proves the validity of the method.

Example 4.4. Consider the system of FDE's

$$\begin{cases} {}^J D^\alpha x = 2y + 3x \\ {}^J D^\alpha y = y - 5x \end{cases}, \ 0 < \alpha \leq 1 \ with \ y(0) = 1, \ x(0) = 2.$$

Let $x(t) = AE_\alpha(\lambda t^\alpha)$ and $y(t) = BE_\alpha(\lambda t^\alpha), \ t > 0$ be its solution.

For the above system, the characteristic equation is:

$$\begin{bmatrix} 3-\lambda & 2 \\ -5 & 1-\lambda \end{bmatrix} = 0.$$

On solving the characteristic equation, we have $\lambda = 2 + 3i, 2 - 3i$.

Then when solving further, the solutions are as follows:

$$x(t) = E_\alpha(2t^\alpha)\Big[2cos_\alpha(3t^\alpha) + 4sin_\alpha(3t^\alpha)\Big],$$
$$y(t) = E_\alpha(2t^\alpha)\Big[cos_\alpha(3t^\alpha) - 5sin_\alpha(3t^\alpha)\Big].$$

This is the exact solution of the above system of the fractional model.

Let $h = T/N$ and $N > 1 \in I$. Let $k = 0, 1, ..., N$ and $x_k = kh$. The exact solution's basis function is $E_\alpha(\lambda t^\alpha)$.

Now, we follow the Micken's rules for establishing NSFD schemes. This fractional linear system can be expressed as follows:

$$\mathbf{w}' = J\mathbf{w}, \tag{4.7}$$

where

$$J = \begin{bmatrix} 2+3i & 0 \\ 0 & 2-3i \end{bmatrix}.$$

The solution for this system is exact finite-difference scheme, which is as follows:

$$\frac{1}{\Phi}(\mathbf{w}_{k+1} - \mathbf{w}_k) = J[\theta \mathbf{w}_{k+1} + (1-\theta)\mathbf{w}_k], \tag{4.8}$$

where $\mathbf{w}_{k+1} = \mathbf{w}(t+h)$ and $\mathbf{w}_k = \mathbf{w}(t)$ and ϕ with θ are defined as follows:

$$\phi = \frac{b\Big(E_\alpha(2ah) + 1 - 2E_\alpha(ah)\ cos(bh))\Big)}{(a^2+b^2)E_\alpha(ah)\ sin(bh)}$$

and

$$\theta = \frac{b + aE_\alpha(ah)\ sin(bh) - bE_\alpha(ah)\ cos(bh)}{b\Big(E_\alpha(2ah) + 1 - 2E_\alpha(ah)\ cos(bh)\Big)}.$$

As the two eigenvalues are complex, $\lambda_1 \neq \lambda_2$, this proves the validity of the method.

5. Convergence analysis of the proposed scheme

In this section we check the consistency and convergence of the numerical schemes. We also compare the error magnitude by using heat maps.

5.1. **Consistency of the numerical scheme.** Here, we formulate and prove the consistency of the numerical scheme.

Theorem 5.1. *Let the system of fractional differential operator D in the linear system is given by*

$$\begin{cases} {}^J D^\alpha[x] = px + qy, \\ {}^J D^\alpha[y] = rx + sy, \end{cases}$$

such that the above system satisfies the following relation

$$\frac{1}{\Phi}(\boldsymbol{w}_{k+1} - \boldsymbol{w}_k) = J[\theta \boldsymbol{w}_{k+1} + (1-\theta)\boldsymbol{w}_k],$$

where J is the Jacobian matrix and Φ, θ are the weight functions defined as in (4.1), (4.2) *and* (4.3). *Then the bound on the Local Truncation Error is given as below:*

$$|LTE_k| \leq \frac{h^\alpha}{\Gamma(1+\alpha)}\left[D^\alpha\big(O(1)\big) + \frac{D^{2\alpha}y(\zeta)}{2}\right],$$

where $\eta, \zeta \in (t_k, t_{k+1})$.

Proof. For the above system, the local truncation error LTE_k is given by the form by Burden and Faires [11]

$$LTE_k = \frac{y_{k+1} - y_k}{\phi(\lambda, h)} + \lambda y_k. \tag{5.1}$$

By adding and subtracting the terms $\frac{y_{k+1}-y_k}{\frac{h^\alpha}{\Gamma(1+\alpha)}}$ and $\alpha y(t_k)$ to the right hand side of (5.1), we get

$$\begin{aligned} |LTE_k| &\leq \left| \frac{y(t_{k+1}) - y(t_k)}{\phi(\alpha, h)} - \frac{y(t_{k+1}) - y(t_k)}{\frac{h^\alpha}{\Gamma(1+\alpha)}} \right| \\ &\quad + \left| \frac{y(t_{k+1}) - y(t_k)}{\frac{h^\alpha}{\Gamma(1+\alpha)})} + \lambda y(t_k) \right| \\ &\leq \left| y(t_{k+1}) - y(t_k) \right| \left| \frac{1}{\phi} - \frac{1}{\frac{h^\alpha}{\Gamma(1+\alpha)}} \right| \\ &\quad + \frac{\frac{h^\alpha \Gamma(1+\alpha)}{\Gamma(1+2\alpha)}}{2} |D^{2\alpha} y(\zeta)|. \end{aligned} \tag{5.2}$$

The quantity $\frac{1}{\phi} - \frac{1}{\frac{h^\alpha}{\Gamma(1+\alpha)}}$ is of $O(1)$. Also, from Taylor expansion,

$$|y(t_{k+1}) - y(t_k)| = \frac{h^\alpha}{\Gamma(1+\alpha)} \dot{y}(\eta), \quad \eta \in [t_k, t_{k+1}],$$

hence (5.2) becomes

$$|LTE_k| \leq \frac{h^\alpha}{\Gamma(1+\alpha)} \left[D^\alpha \big(O(1)\big) + \frac{D^{2\alpha} y(\zeta)}{2} \right], \tag{5.3}$$

where $\eta, \zeta \in (t_k, t_{k+1})$.

From equation (5.3), we find that as $h \to 0$, $|LTE_k| \to 0$ which proves the consistency of the numerical scheme (4.8). □

5.2. **Numerical experiments and their convergence.** Based on our calculations from the above section for the exact analytical solutions, we implement the NSFDS and compare the outcomes in the following. We also discuss the error magnitude using the heat maps as follows:

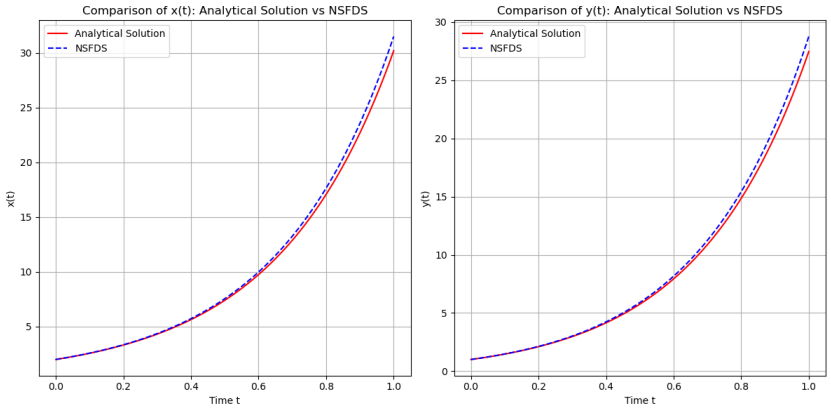

FIGURE 1. Error comparison between $y(t)$ and $x(t)$ for Example 1.

In Figure 1, a comparison between the analytical solution and the numerical solution using the NSFD scheme for $x(t)$ and $y(t)$ over the interval $t \in [0, 1]$, is shown. The NSFDS stays close to the analytical solution throughout most of the interval, indicating the exponential growth pattern of both $x(t)$ and $y(t)$. However, as t approaches 1, a slight divergence becomes visible, with the NSFDS solution slightly underestimating the analytical solution. Overall, both solutions stay very close in the start and mid of the interval, suggesting that NSFDS provides an accurate approximation of the analytical solution, with only minor errors occurring towards the end. Below, we present error comparison in tabular data.

TABLE 1. Error comparison between y(t) and x(t) for Example 1 by using exact and NSFDS.

t	$x-exact$	$x-NSFDS$	$x-error$	$y-exact$	$y-NSFDS$	$y-Error$
0.00	2.00	2.00	0.00	1.00	1.00	0.0
0.10	2.57737367	2.576436928	9.36742E-04	1.472202752	1.47132123	8.81522E-04
0.20	3.34387958	3.341364704	2.51488E-03	2.122476822	2.120083998	2.39282E-03
0.30	4.364334071	4.359265496	5.06857E-03	3.014475263	3.009609017	4.86625E-03
0.40	5.726087733	5.717000268	9.08746E-03	4.234263035	4.225473707	8.78933E-03
0.50	7.546894241	7.531609732	1.52845E-02	5.89817297	5.883300316	1.48727E-02
0.60	9.985530597	9.960838237	2.46924E-02	8.163411796	8.139265626	2.41462E-02
0.70	13.25613122	13.21733142	3.87998E-02	11.24237852	11.20428294	3.80956E-02
0.80	17.64753504	17.58779053	5.97445E-02	15.42199411	15.36313905	5.88551E-02
0.90	23.54939914	23.45881431	9.05848E-02	21.08979603	21.00031704	8.94790E-02
1.00	31.4874463	31.3517639	1.35682E-01	28.76916447	28.63483997	1.34325E-01

Here, we give error heat maps:

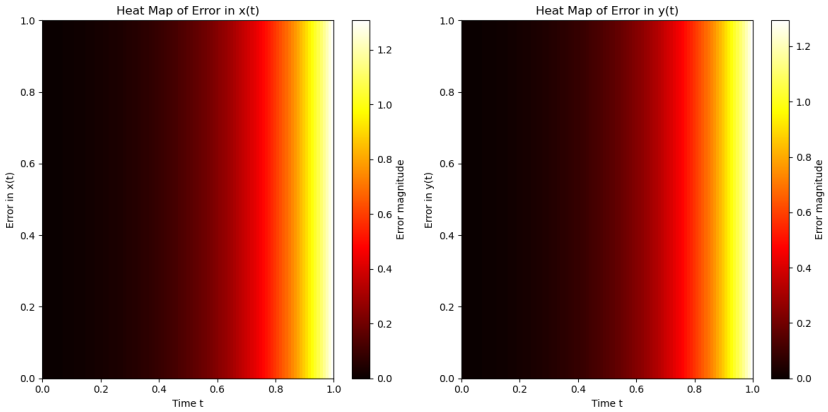

FIGURE 2. Heat map for error magnitude for $y(t)$ and $x(t)$ for Example 1.

Figure 2 shows heat maps for the error magnitude in $x(t)$ and $y(t)$ over the time interval $t \in [0, 1]$. From $t = 0$ to approximately $t = 0.6$, the error magnitude is very low, within the range of 0 to 0.2, as shown by the darker regions in the heat maps. Between $t = 0.6$ and $t = 0.8$, the error gradually increases, with values reaching around 0.4. The error increases from $t = 0.8$ to $t = 1.0$, where the magnitude reaches up to 1.2. This increase suggests that the NSFDS approximation deviates more noticeably from the analytical solution toward the end of the interval. Overall, the error remains minimal and a good approximation is obtained.

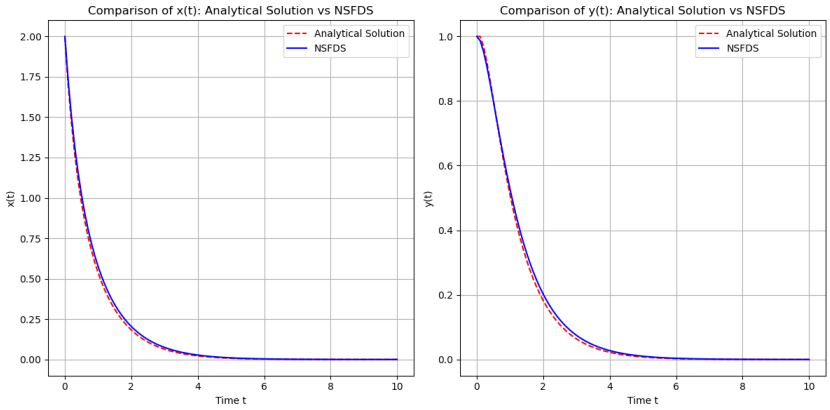

FIGURE 3. Error comparison between y(t) and x(t) for Example 2.

Figure 3 shows that in both graphs, the NSFDS approximation stays close to the analytical solution over the whole time interval. From $t = 0$ to $t = 2$, both $x(t)$ and $y(t)$ exhibit a steep decline, with $x(t)$ decreasing from its initial value of 2 and $y(t)$ from 1. Between $t = 2$ and $t = 5$, the rate of decline in $x(t)$ and $y(t)$ slows, and both solutions approach lower values. From $t = 5$ to $t = 10$, both $x(t)$ and $y(t)$ converge toward zero, stabilizing at very low values. Below, we present error comparison in tabular data.

TABLE 2. Error comparison between y(t) and x(t) for Example 2 by using exact and NSFDS.

t	$x-exact$	$x-NSFDS$	$x-error$	$y-exact$	$y-NSFDS$	$y-Error$
0.00	2.00	2.00	0.00	1.00	1.00	0.00
1.00	0.572824766	0.576712697	3.88793E-03	0.525272258	0.526925627	1.65337E-03
2.00	0.202100133	0.204242301	2.14217E-03	0.199838892	0.201763549	1.92466E-03
3.00	0.073615105	0.074742307	1.12720E-03	0.073507577	0.074618898	1.11132E-03
4.00	0.026928387	0.02747653	5.48144E-04	0.026923273	0.027470386	5.47113E-04
5.00	0.009855846	0.010107073	2.51227E-04	0.009855603	0.010106768	2.51165E-04
6.00	0.00360752	0.003718136	1.10616E-04	0.003607508	0.003718121	1.10612E-04
7.00	0.001320467	0.001367823	4.73563E-05	0.001320466	0.001367823	4.73561E-05
8.00	0.000483334	0.000503194	1.98604E-05	0.000483334	0.000503194	1.98604E-05
9.00	0.000176916	0.000185115	8.19900E-06	0.000176916	0.000185115	8.19900E-06
10.00	0.00006476	0.00006810	3.34302E-06	0.00006476	0.00006810	3.34302E-06

Here, we give error heat maps:

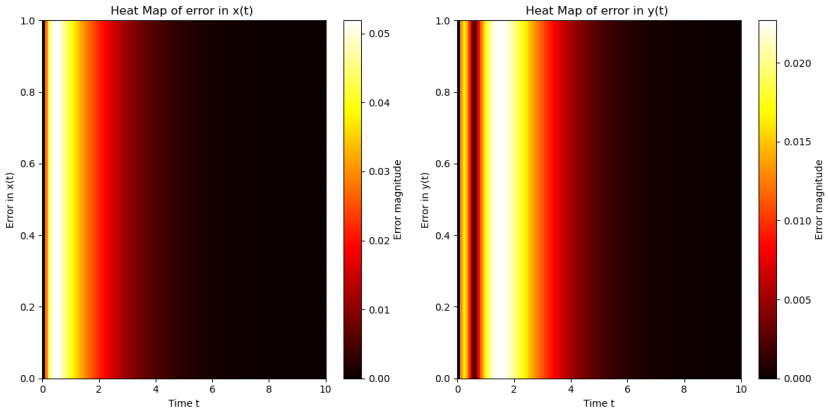

FIGURE 4. Heat map for error magnitude for $y(t)$ and $x(t)$ for Example 2.

Figure 4 shows heat maps for the error magnitude in $x(t)$ and $y(t)$. From $t = 0$ to approximately $t = 2$, the error is small, with values close to zero.

From time $t = 2$ to $t = 5$, the error magnitude slightly increases, reaching around 0.02 for $y(t)$ and 0.04 for $x(t)$. In the interval from $t = 5$ to $t = 10$, the error remains relatively stable at a low magnitude, suggesting that NSFDS maintains accuracy over a longer time span.

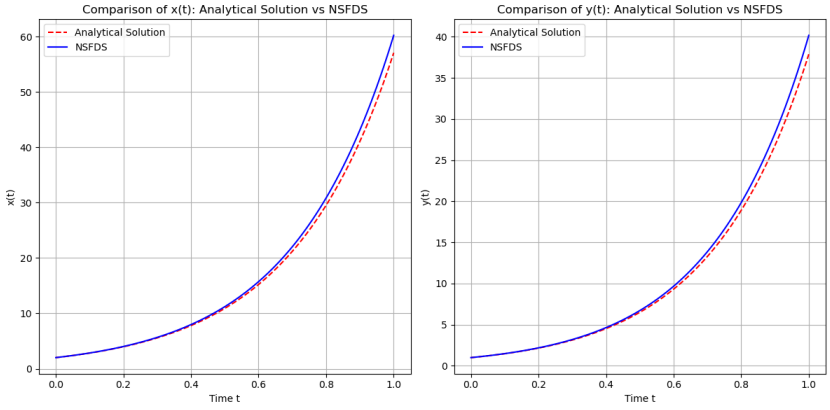

FIGURE 5. Error comparison between $y(t)$ and $x(t)$ for Example 3.

Figure 5 shows a comparison between the analytical solution and the NSFDS approximation for $x(t)$ and $y(t)$. As t approaches 1, the NSFDS approximation shows a little deviation. This deviation is consistent also at higher values, around $t = 1$, where $x(t)$ reaches approximately 60 and $y(t)$ reaches around 40. The close alignment of both solutions in the early stages and their gradual divergence near $t = 1$ indicate that the NSFDS maintains good accuracy initially but accumulates minor errors towards the end of the interval. Below, we present error comparison in tabular data.

TABLE 3. Error comparison between y(t) and x(t) for Example 3 by using exact and NSFDS.

t	$x-exact$	$x-NSFDS$	$x-error$	$y-exact$	$y-NSFDS$	$y-Error$
0.00	2.00	2.00	0.00	1.00	1.00	0.00
0.10	1.70000000	1.72767500	2.76750E-02	1.00000000	0.98683750	1.31625E-02
0.20	1.46000000	1.50251645	4.25165E-02	0.97000000	0.95367625	1.63237E-02
0.30	1.26500000	1.31452833	4.95283E-02	0.92200000	0.90792693	1.40731E-02
0.40	1.10420000	1.15609322	5.18932E-02	0.86410000	0.85486765	9.23235E-03
0.50	0.96977000	1.02137600	5.16060E-02	0.80170000	0.79821680	3.48320E-03
0.60	0.85598600	0.90588025	4.98943E-02	0.73833700	0.74055555	2.21855E-03
0.70	0.75862250	0.80611780	4.74953E-02	0.67626820	0.68363906	7.37086E-03
0.80	0.67452482	0.71936236	4.48375E-02	0.61687681	0.62862551	1.17487E-02
0.90	0.60130754	0.64346561	4.21581E-02	0.56095393	0.57624436	1.52904E-02
1.00	0.53714142	0.57671967	3.95783E-02	0.50889390	0.52691965	1.80258E-02

Here, we give error heat maps:

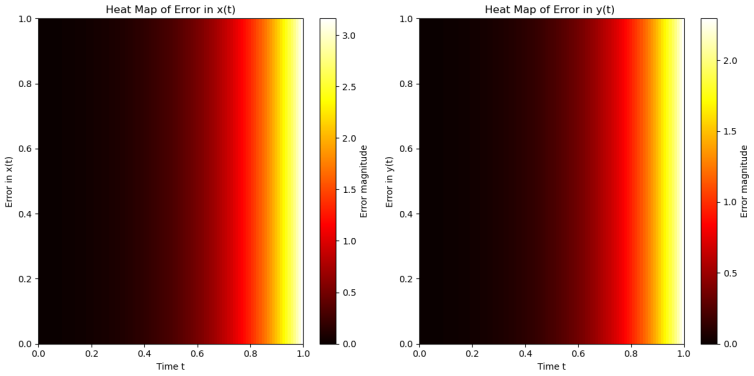

FIGURE 6. Heat map for error magnitude for $y(t)$ and $x(t)$ for Example 3.

Figure 6 shows error magnitudes using heat maps. From time $t = 0$ to approximately $t = 0.6$, the error remains relatively low, staying below 0.5. As t progresses from 0.6 to 0.8, the error magnitude begins to increase, reaching values around 1.0 for both $x(t)$ and $y(t)$. In the end region from $t = 0.8$ to $t = 1.0$, the error increases, with $x(t)$ reaching around 3.0 and $y(t)$ around 2.0. The graphs suggest that the NSFDS approximation performs better in the initial portion of the interval but accumulates some error, though not significant, as t approaches 1.

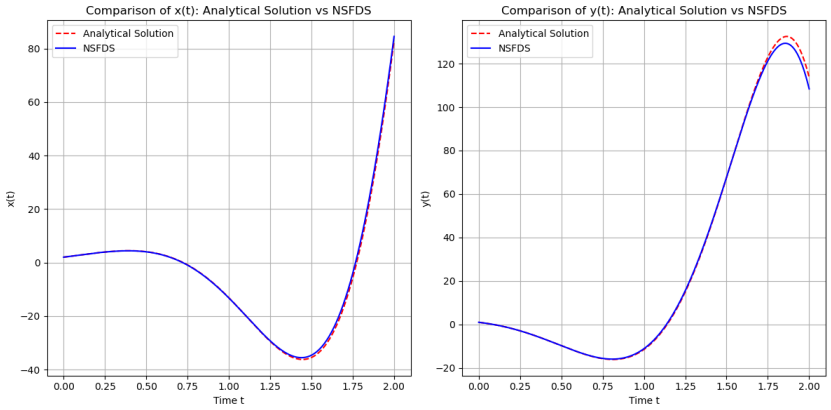

FIGURE 7. Error comparison between $y(t)$ and $x(t)$ for Example 4.

Figure 7 shows that from time $t = 0.5$ to $t = 1.5$, the solutions for both $x(t)$ and $y(t)$ achieve negative values before rising towards the end of the interval. The NSFDS shows a slight deviation from the analytical solution in this region, with small discrepancies noticeable near the highest and lowest points, but it remains close to the analytical solution. As t approaches 2, both $x(t)$ and $y(t)$ reach higher values. Below, we present error comparison in tabular data.

TABLE 4. Error comparison between y(t) and x(t) for Example 4 by using exact and NSFDS.

t	$x-exact$	$x-NSFDS$	$x-error$	$y-exact$	$y-NSFDS$	$y-Error$
0.00	2.00	2.00	0.00	1.00	1.00	0.00
0.20	1.49875758	1.50250195	3.74437E-03	0.95496323	0.95369031	1.27292E-03
0.40	1.15131378	1.15607718	4.76339E-03	0.85560149	0.85488296	7.18532E-04
0.60	0.90113830	0.90586690	4.72860E-03	0.74033163	0.74056801	2.36380E-04
0.80	0.71500770	0.71935242	4.34472E-03	0.62756194	0.62863447	1.07253E-03
1.00	0.57282477	0.57671270	3.88793E-03	0.52527226	0.52692563	1.65337E-03
1.20	0.46199998	0.46545318	3.45320E-03	0.43614119	0.43812946	1.98826E-03
1.40	0.37432888	0.37739323	3.06436E-03	0.36026702	0.36239766	2.13064E-03
1.60	0.30423892	0.30695965	2.72073E-03	0.29659216	0.29872990	2.13774E-03
1.80	0.24779109	0.25020662	2.41554E-03	0.24363282	0.24569004	2.05722E-03
2.00	0.20210013	0.20424230	2.14217E-03	0.19983889	0.20176355	1.92466E-03

Here, we give error heat maps:

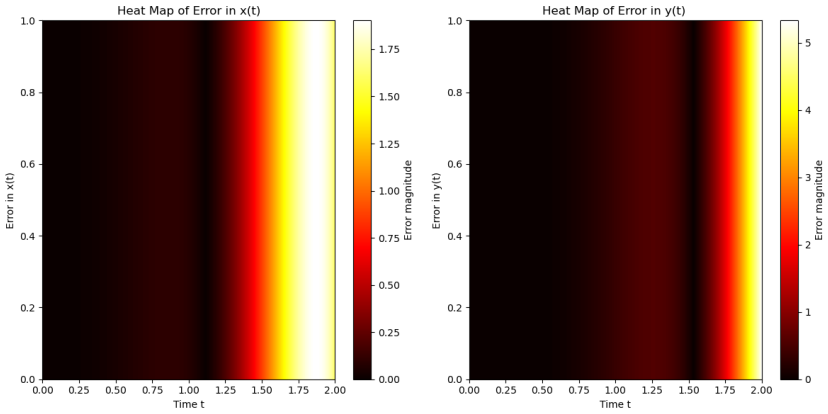

FIGURE 8. Heat map for error magnitude for $y(t)$ and $x(t)$ for Example 4.

Figure 8 shows heat maps over the interval $t \in [0, 2]$. From $t = 0$ to around $t = 1$, the error remains small. The error starts increasing around $t = 1$ and attains higher values by the time $t = 1.5$. In the last region, from $t = 1.5$ to $t = 2$, the error magnitude reaches its maximum, with values reaching to approximately 1.75 for $x(t)$ and around 5 for $y(t)$.

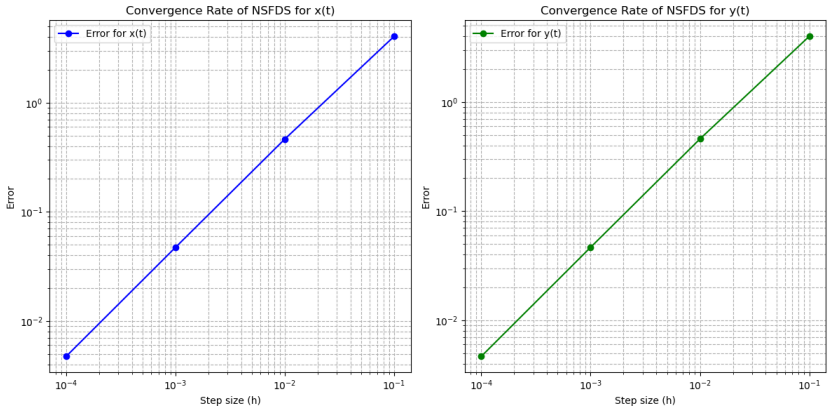

FIGURE 9. Rate of Convergence in $y(t)$ and $x(t)$ for Example 1.

Figure 9 shows the convergence rate of the NSFDS for $x(t)$ and $y(t)$, the error is considered as a function of the step size h. For the relatively larger step size $h = 0.1$, the error for $x(t)$ is approximately 10^{-1} and for $y(t)$ around 10^{0}. As the step size is reduced to $h = 0.01$, the error decreases to roughly 10^{-2} for $x(t)$ and 10^{-1} for $y(t)$. Further reducing the step size to $h = 0.001$

results in an error close to 10^{-3} for $x(t)$ and 10^{-2} for $y(t)$. At the smallest step size, $h = 0.0001$, the error falls to approximately 10^{-4} for $x(t)$ and 10^{-3} for $y(t)$. The convergence almost depicts a linear rate in both plots and confirms that the error decreases consistently with smaller step sizes, highlighting a predictable rate of convergence for NSFDS. This pattern demonstrates that NSFDS effectively reduces errors as the step size is refined, reinforcing its accuracy and reliability for approximating $x(t)$ and $y(t)$ with improved discretization.

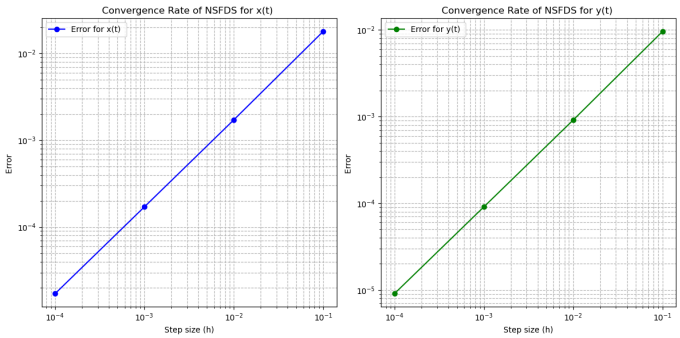

FIGURE 10. Rate of Convergence in $y(t)$ and $x(t)$ for Example 2.

The convergence rate in Figure 10 shows that for the step size $h = 0.1$, the error for $x(t)$ and $y(t)$ is around 10^{-2}. As the step size decreases to $h = 0.01$, the error reduces for both $x(t)$ and $y(t)$ to approximately 10^{-3}. As we decrease the step size, the error further decreases to about 10^{-4} for $x(t)$ and $y(t)$. Lastly, at the smallest step size, $h = 0.0001$, the error is as low as 10^{-5} for both $x(t)$ and $y(t)$.

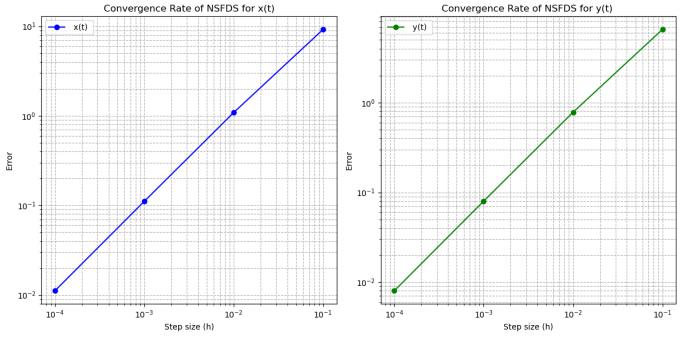

FIGURE 11. Rate of Convergence in $y(t)$ and $x(t)$ for Example 3.

The convergence rate in Figure 11 shows that for the step size $h = 0.1$, the error for $x(t)$ and $y(t)$ is approximately 10^{-1}. As the step size is reduced to $h = 0.01$, the error decreases to around 10^{-2} for both $x(t)$ and $y(t)$. With a further reduction to $h = 0.001$, the error drops to roughly 10^{-3} for both functions. Finally, at $h = 0.0001$, the error reaches about 10^{-4} for both $x(t)$ and $y(t)$.

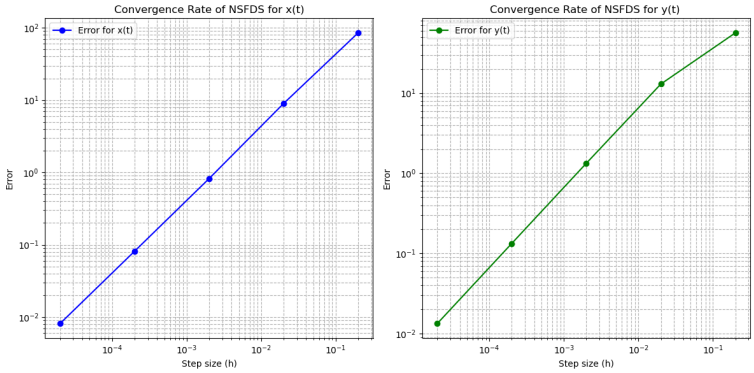

FIGURE 12. Rate of Convergence in $y(t)$ and $x(t)$ for Example 4.

The convergence rate in Figure 12 shows that for the the step size $h = 0.1$, the error for $x(t)$ is around 10^{-1}, and for $y(t)$, it is slightly lower at around 10^{-1}. As the step size is reduced to $h = 0.01$, the error for both functions decreases to about 10^{-2}. For $h = 0.001$, the error further decreases to approximately 10^{-3} for both $x(t)$ and $y(t)$. At the smallest step size, $h = 0.0001$, the error reaches roughly 10^{-4} for both the state variables.

6. Conclusion

Using the modified fractional derivative and the Mittag-Leffler function, the NSFDS solves the system of FDE's. It is evident from the numerical simulations that the exact solution's efficiency is accurate. By using Mittag-Leffler, as we have shown in this research, the application of this type of fractional Jumarie derivative provides a conjugation with traditional approaches in order to solve a system of linear integer order differential equations. Researchers studying fractional dynamic systems find this approach appealing due to its simplicity compared to the standard method to get the solution of linear FDE's. These numerical computations show that the NSFDS approximation performs well and stays close to the analytical solution. The heat maps also illustrate how the error is kept within a suitable range over time, highlighting regions and deviations for the NSFDS approximation and the analytical solutions.

Acknowledgments: The first author would like to extend his appreciation to the Ministry of Higher Education, Research and Innovation, Oman for funding this work under Block Funding Project (2024-25).

References

[1] O. Abdulaziz, I. Hashim, S. Momani, *Application of homotopy-perturbation method to fractional IVPs,* J. Comput. Appl. Math.,**216** (2008) 574–584.

[2] S. Ali and E. Bashier. *Nonstandard Finite Difference Schemes for Solving Systems of two Linear Fractional Differential Equations*, Stat. Optim. Inform. Comput., **14(4)**(2025), 2041-2060. doi.org/10.19139/soic-2310-5070-2564.

[3] S.S. Al-Kathiri, F. Abdullah, N.N. Hamid, E. Bashier, A.A. Bhat and D.A. Sunny, *Applications of the Nonstandard Finite Difference Method to a Fractional Model Explaining Diabetes Mellitus and Its Complications*, Contemporary Math., **5**(4) (2024), 6296–6319.

[4] S. Al-Shanfari, D.A. Sunny, I.M. Elmojtaba, N. Al-Salti and S. Pushpan, *A delay mathematical model for cholera transmission: Stability, chaos and bifurcation*, Chaos, Solitons Fract., **198**(7217) (2025), 116464.

[5] J. Ayub, D.A. Sunny and M. Aqeel, *A new hyperchaotic system with Hopf bifurcation and its boundedness: infinite coexisting hidden and self-excited attractor*, Soft Computing, **27**(2) (2023), 887–901.

[6] D. Baleanu, S. Zibaei, M. Namjoo and A. Jajarmi, *A nonstandard finite difference scheme for the modeling and non identical synchronization of a novel fractional chaotic system*, Adv. Diff. Equ., **2021**(1) (2021).

[7] E.B.M. Bashier, *Practical Numerical and Scientific Computing with MATLAB and Python*, CRC Press, Boca Raton, (2020). DOI:10.1201/9780429021985.

[8] S. Bhalekar and V. Daftardar-Gejji, *Solving fractional-order logistic equation using a new iterative method*, Int. J. Diff. Equ., (2012), 1-12.

[9] A.A. Bhat, J.A. Ganie, M.Y. Bhat and F.B.A. Sulaiman, *Generating Operators of I-Transform of the Mellin Convolution Type*, J. Appl. Math. Infor., **42**(1) (2024).

[10] A.A. Bhat, H.A. Rizvi, J.A. Ganie, F.B A. Sulaiman, M.Y. Bhat and D.K. Jain, *Differential Transform Method for Solving Volterra q-Integral Equations*, Contemporary Math., (2023), 1222–1233.

[11] R.L. Burden and J.D. Faires, *Numerical Analysis, 9th Edition, Brookscole*, Boston, 2011.

[12] M. Caputo, *Linear models of dissipation whose q is almost frequency independent*, Geophysical J. Royal Astronomical Soc., **13**(5) (1967), 529–539.

[13] M. Dalir and M. Bashour, *Applications of fractional calculus*, Appl. Math. Sci., **4**(21) (2010), 1021-1032.

[14] S. Das, *Functional Fractional Calculus 2nd Edition*, Springer-Verlag, 2011.

[15] K. Diethelm, *The analysis of Fractional Differential equations*, Springer-Verlag, 2010.

[16] K. Diethelm, N.J. Ford and A.D. Freed, *A predictor-corrector approach for the numerical solution of fractional differential equations*, Nonlinear Dynamics, **29** (2002), 3–22.

[17] K. Diethelm and W. Guido, *Numerical solution of fractional order differential equations by extrapolation*, Numer. Algo., **16**(3) (1997), 231–253.

[18] A. Erdelyi, *Asymptotic expansions*, Dover 1954.

[19] A. Erdelyi, *(Ed). Tables of Integral Transforms*, **1**, McGraw-Hill, 1954.

[20] A. Erdelyi, *On some functional transformation*, Univ Potitec Torino, 1950.

[21] V.S. Ertürk and S. Momani, *Solving systems of fractional differential equations using differential transform method*, J. Compu. Appl. Math., **215** (2008), 142–151.

[22] N. Gauss, G. Schneider, D.A. Sunny and D. Zimmermann, *Modulation theory for pattern forming systems with a spatial 1:2-resonance*, Chaos: An Interdisciplinary J. Nonlinear Sci., **31**(5) (2021), 053–109.

[23] U. Ghosh, S. Sarkar and S. Das, *Solution of system of linear fractional differential equations with modified derivative of Jumarie type*, Amer. J. Math. Anal., **3**(3) (2015), 72–84.

[24] U. Ghosh, S. Sengupta, S. Sarkar and S. Das, *Characterization of non-differentiable points of a function by Fractional derivative of Jumarie type*, European Journal of Academic Essays, **2**(2) (2015), 70–86.

[25] U. Ghosh, S. Sengupta, S. Sarkar and S. Das, *Analytic solution of linear fractional differential equation with Jumarie derivative in terms of Mittag-Leffler function*, Amer. J. Math. Anal., **3**(2) (2015), 32–38.

[26] M. Hajipour, A. Jajarmi and D. Baleanu, *An efficient nonstandard finite difference scheme for a class of fractional chaotic systems*, J. Comput. Nonlinear Dyna., **13**(2) (2017).

[27] Y. Hua, Y. Luoa and Z. Lu, *Analytical solution of the linear fractional differential equation by Adomian decomposition method*, J. Comput. Appl. Math., **215** (2008), 220–229.

[28] G. Jumarie, *Modified Riemann-Liouville derivative and fractional Taylor series of non-differentiable functions Further results*, Comput. Math. Appl., **51** (2006), 1367–1376.

[29] A. Kilbas, H.M. Srivastava and J.J. Trujillo, *Theory and Applications of Fractional Differential Equations. North-Holland Mathematics Studies*, Elsevier Sci. Amsterdam, the Netherlands, **204** (2006).

[30] R. Metzler and J. Klafter, *The random walk's guide to anomalous diffusion: a fractional dynamics approach*, phys. Rep., **339** (2000), 1–77.

[31] R.E. Mickens, *Advances in the Applications of Nonstandard Finite Difference Schemes*, World Scientific Publishing Danvers, 2005.

[32] R.E. Mickens, *Nonstandard Finite Difference Models of Differential Equations*, World Scientific, New Jersey, 1993.

[33] R.E. Mickens, *Applications of Nonstandard Finite Difference Schemes*, World Scientific, New Jersey, 2000.

[34] R.E. Mickens, K. Oyedejib and S. Rucker, *Exact finite difference scheme for second-order, linear ODEs having constant coefficients*, J. Sound Vibration, **287** (2005), 1052-1056.

[35] K.S. Miller and B. Ross, *An Introduction to the Fractional Calculus and Fractional Differential Equations*, John Wiley and Sons, New York, NY, USA; 1993.

[36] M.G. Mittag-Leffler, *Sur la nouvelle function E(x)*, Comptes Rendus Acad. Sci, Paris (Ser.II)**137** (1903), 554–558.

[37] K. Moaddy, I. Hashim and S. Momani, *Non-standard finite difference schemes for solving fractional-order rossler chaotic and hyper chaotic systems*, Comput. Amp math Semicolon Math. Appl., **62**(3) (2011), 1068-1074.

[38] M.Y. Ongun, D. Arslan and R. Garrappa, *Nonstandard finite difference schemes for a fractional-order brusselator system*, Adv. Difference Equ., **1** (2013).

[39] A. Pathak, R. Mishra, D.K. Jain, F. Ahmad and A.A. Bhat, *Certain results of Aleph-Function based on natural transform of fractional order*, Ann. Math. Phys., **6**(1) (2023), 052–057. doi.org/10.17352/amp.000078.

[40] K.C. Patidar, *On the use of nonstandard finite difference methods*, J. Diff. Equ. Appl. **11** (2005), 735-758.

[41] I. Podlubny, *Fractional Differential Equations, Mathematics in Science and Engineering*, Academic Press, San-Diego, Calif. USA, **198** 1999.
[42] T.R. Prabhakar, *A singular integral equation with a generalized Mittag-Leffler function in the kernel*, Yokohama Math. J. **19** (1971), 7–15.
[43] K. Rajput, R. Mishra, D.K. Jain, A.A. Bhat and F. Ahmad, *The fractional integral inequalities involving Kober and SaigoMaeda operators*, Commun. Adv. Math. Sci., **3**(6) (2023), 135–141.
[44] S.S. Ray and R.K. Bera, *An approximate solution of a nonlinear fractional differential equation by Adomian decomposition method*, Appl. Math. Comput., **167** (2005), 561–571.
[45] S.Z. Rida and A.A.M. Arafa, *New method for solving linear fractional differential equations*, Int. J. Diff. Equ., (2011), 1-8.
[46] L.I.W. Roeger, *Exact finite-difference schemes for two-dimensional linear systems with constant coefficients*, J. Comput. Appl. Math., **219**(1) (2008), 102–109.
[47] L.I.W. Roeger, *Exact nonstandard finite-difference methods for a linear system the case of centers*, J. Diff. Equ. Appl., **14**(4) (2008), 381-389.
[48] B. Wang, L. Li and Y. Wang, *An efficient nonstandard finite difference scheme for chaotic fractional-order chen system*, IEEE Access, **8** (2020), 98410-98421.
[49] R. Yulita Molliq, M.S.M. Noorani, I. Hashim and R.R. Ahmad, *Approximate solutions of fractional ZakharovKuznetsov equations by VIM*, J. Comput. Appl. Math., **233**(2) (2009), 103–108.
[50] S.S. Zeid, *Approximation methods for solving fractional equations*, Chaos, Solitons Amp Mathsemicolon Fract., **125** (2019), 171-193.